THE CRYOGENIC APPROACH TO SIMULATING HOT JET IN TRANSONIC WIND-TUNNEL TESTING

Keisuke ASAI

National Aerospace Laboratory

Tokyo, Japan

Abstract

A novel approach to the hot-jet simulation problems in transonic wind-tunnel testing is presented. This technique utilizes the advantages of cryogenic temperatures in wind-tunnel testing. Theoretical considerations show that in a cryogenic wind tunnel hot jet can be simulated by using a test gas at ambient or moderately elevated temperatures. It is also shown that, through use of a mixture of nitrogen and methane as a jet gas, complete simulation of the full-scale turbojet exhaust becomes possible in a cryogenic tunnel. In order to validate this concept, a series of experiments were conducted in the NAL 0.1m Transonic Cryogenic Wind Tunnel. A blunt-based afterbody model was used to evaluate the jet temperature effect on the base pressure. A good qualitative agreement was found between the results obtained from the cryogenic approach and the previous hot-jet data. By varying jet gas composition and temperature separately, the independent effects of jet temperature ratio, specific heat ratio, and molecular weight (gas constant) on the base pressure have been determined. It has been verified that the effect of gas constant on the jet entrainment is equivalent to that of jet temperature.

Nomenclature

C_p	pressure coefficient, $(p-p_0)/q_0$
d	diameter, m
L	linear dimension, m
$\dot{m}$	mass-flow rate, kg/sec
M	Mach number
p	pressure, kPa
Pr	Prandtl number
q	dynamic pressure, kPa
R	gas constant, J/kg-K
Re	Reynolds number
T	temperature, K
V	velocity, m/sec
x	mass fraction
γ	the ratio of specific heats
ρ	density, kg/m^3

Subscripts:

0	free stream (sometimes omitted)
b	base
d	model diameter
j	jet flow
L	LN2 injection
t	stagnation

Abbreviations:

C/P	combustion products
NPR	nozzle pressure ratio, p_{tj}/p_0
TR	jet temperature ratio, T_{tj}/T_{t0}

1. Introduction

Insufficient capabilities of existing aerodynamic testing techniques have sometimes caused serious problems in the development of jet airplanes. Among these problems, the effects of Reynolds number, wall interference, and support interference are regarded as being most important. A realistic simulation of the effects of turbojet exhausts is also important particularly when integration of propulsion system with airframe is a critical factor in the aircraft design. A combustion gas exhausted from a turbojet engine is as hot as 1000 Kelvin or even higher temperatures for afterburning conditions. Regardless of this fact, the effects of jet temperature are usually ignored and a wind-tunnel test is mostly performed by using a cold compressed air to represent a jet exhaust.

The effects of jet temperature are known to be important in some critical aerodynamic phenomenon. One of the most well-known problems is that associated with aircraft afterbody design (Ref.1). Pressure drag acting on the afterbody is very sensitive to jet temperature, particularly at transonic Mach numbers and for separated flows. In some cases, a cold air test results in a very pessimistic drag prediction, that is, up to 35 % of the jet-off afterbody drag. In the previous studies on jet-temperature effects (Refs. 2, 3 and 4), a hydrogen peroxide (H_2O_2) technique or an ethylene/air combustion technique was used to simulate realistic turbojet exhausts. With these techniques, jet temperatures higher than 1000 Kelvin can be attained. However, it is unlikely that these techniques are used in a routine test because they require an extremely complex and costly model.

As a solution to this frustrating problem, the author has proposed in Ref.5 a novel hot-jet simulation technique, which utilizes the advantages of cryogenic temperatures in wind-tunnel testing. Theoretical considerations given in Ref.5 showed that in a cryogenic wind tunnel the effects of hot jet could be simulated by using a test gas at ambient or slightly elevated temperatures. It was also shown that, through use of a mixture of nitrogen and methane as a jet gas, a perfect simulation of the full-scale turbojet exhaust would be possible in a cryogenic wind tunnel. Even with a subscale model, all the relevant scaling parameters including jet temperature ratio, jet velocity ratio, ratio of specific heats, Reynolds number, and Mach number can be matched to the full-scale flight values.

Copyright © 1992 by ICAS and AIAA. All rights reserved.

In order to validate this concept, an experimental investigation was conducted in the NAL 0.1m Transonic Cryogenic Wind Tunnel. A blunt-based cylindrical afterbody model was used as a test article to assess the effects of jet gas properties on the base pressure. For a realistic simulation of turbojet flow, a mixture of nitrogen and methane at ambient and moderately-elevated temperatures was used as a jet gas. The obtained results were then compared with the previous hot-jet data obtained by NACA using an ethylene/air combustor in an atmospheric ambient-temperature tunnel.

In addition to the verification tests, a fundamental research on the effects of jet gas properties on the base flow was also conducted in the NAL 0.1m TCWT. In contrast with the conventional jet-simulation techniques, the cryogenic approach can offer a unique testing capability which allows us to determine separate effects of jet temperature ratio, specific heat ratio, and molecular weight (gas constant). In order to alter the thermodynamic properties of a jet gas, different mixtures of nitrogen and either of methane, argon, or helium were used. And, gas temperature was also varied to cover the wide range of jet-temperature ratio.

In this paper, the theoretical background of the cryogenic approach is first reviewed briefly and then the experimental results obtained in the NAL 0.1m TCWT are presented. The latter includes some of the results obtained at the first series of experiments, which have been already reported in Ref.6. However, the main portion of this paper consists of the results obtained in the second series of experiments, which were performed early in 1992.

2. Theoretical Background

2.1 Similarity Rule

The interacting flow field of the jet exhaust and the external flow is governed by the Navier-Stokes equation system. Similarity parameters relevant to jet-flow interaction can be derived by nondimensionalizing the field equations and the boundary conditions. Assuming the geometrical similarity, the following twelve scaling parameters can be derived from the basic equations;

Group 1 (simulation of external flow);
M_0; Re_0; γ_0; Pr_0

Group 2 (simulation of internal flow);
M_j; Re_j; γ_j; Pr_j

Group 3 (simulation of interaction);
p_j/p_0; T_j/T_0; V_j/V_0; L_j/L_0

Scaling parameters such as mass flow ratio, momentum ratio, and internal energy ratio, which have been frequently used to correlate the jet interaction effects, can be derived by combining the above parameters.

2.2 Use of N_2/CH_4 as a Jet Gas (Ref.5 and Ref.7)

As a datum for evaluating the jet-simulation accuracy of the cryogenic technique, thermodynamic properties of the combustion products were calculated assuming a hypothetical single-spool turbojet engine. The jet fuel used in the calculation is hydrocarbon having the H/C atom ratio of 2. The calculated composition of the combustion products is given in Table 1 for both non-afterburning and afterburning conditions.

Afterburner		OFF	ON
Temperature, K (T_{tj}/T_{to})		1000 (3.33)	1500 (5.00)
γ_j		1.322	1.286
Molecular Weight		28.95	28.93
Mol Fraction	CO_2	0.040	0.071
	H_2O	0.040	0.070
	N_2	0.765	0.753
	O_2	0.145	0.096
	Ar	0.009	0.009

Table 1 Composition of Combustion Products

As shown in Table 1, the value of γ for the combustion gas is much smaller than the ideal diatomic value (1.4). By contrast, air and nitrogen behave like an ideal diatomic gas over the wide range of pressure and temperature. So, for a realistic turbojet simulation, we have to reduce the value of γ. To reduce γ, we have to use polyatomic gases. Among all the candidate gases, methane gas was found suitable for use in cryogenic wind-tunnel testing. Methane has a relatively low boiling temperature (111.6K at 1.0bar) and therefore we can make full use of the high Reynolds number capability of the cryogenic wind tunnel. The desired value of γ can be matched by adjusting the mol fraction of methane in the nitrogen-based test gas.

Figures 1(a) and 1(b) compares the jet-simulation capabilities of the cryogenic approach with those of a conventional cold-air technique for both non-afterburning and afterburning conditions. The polygon shown in these figures is composed of the similarity parameters normalized by the values estimated for the full-scale turbojet conditions (Table.1). The closer the polygon is to a complete circle, the more accurate the simulation is. As is clearly seen in these figures, the jet-flow simulation of the cryogenic approach is practically perfect. This is contrast with that a conventional cold-air method has several deficiencies in flow simulation.

The isentropic pressure ratio, p/p_t, expressed as a function of the expansion Mach number, is presented in Figs. 2(a) and 2(b) for non-afterburning and afterburning conditions, respectively. These calculations were made using the Beattie-Brigeman equation of state to account for real-gas effects of a N_2/CH_4 mixture. The ordinate in these figures is normalized by the reference value obtained for an ideal diatomic gas (γ=1.4). The curves for the real combustion gases are also shown as dashed lines. As is seen, a N_2/CH_4 mixture can simulate very well the behaviour of the real combustion gas. This statement is true for the other isentropic flow parameters and normal shock parameters. See Ref.7 for details.

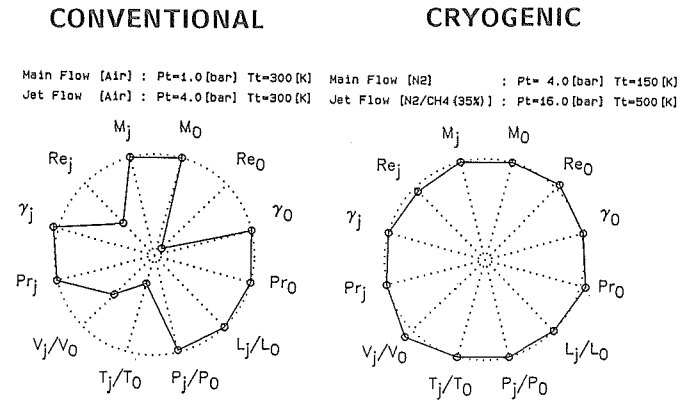

(a) non-afterburning case

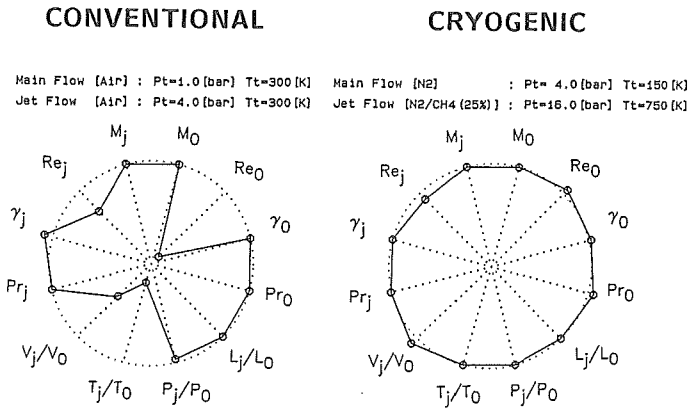

(b) afterburning case

Fig. 1 Comparison of jet-simulation capabilities

2.3 Flow Contamination Effect (Ref.7)

When a jet gas is blown in a continuous wind tunnel, the problem of flow contamination occurs. In an atmospheric wind tunnel, a great amount of air should be exchanged with the atmosphere to keep the tunnel flow clean. Some propulsion tunnels are equiped with a scavenging scoop to capture the combustion gas, but this method is not suitable when the model angles of attack is varied over the wide range.

Use of a N_2/CH_4 jet gas in a cryogenic wind tunnel also causes the problem of free-stream contamination. The contamination effect due to mixing of the tunnel flow and methane has been assessed in Ref.7. The mol fraction of CH_4 in the free stream increases with time until the amount of methane injected into the tunnel balances the amount of methane discharged from the tunnel. An equilibrium value of the mass fraction of CH_4 in the tunnel flow can be obtained as $x_0 = x_j\dot{m}_j/(\dot{m}_L + \dot{m}_j)$, where x denotes mass fraction of methane and $\dot{m}$ represents mass flow. The subscripts, 0, j, L correspond to free-stream, jet, and injected LN_2, respectively.

This equation indicates that in a cryogenic wind tunnel the mass fraction of methane for the free stream (x_0) is smaller by an order than that for a jet gas (x_j), since a large amount of liquid nitrogen is continuously injected into the tunnel to remove the heat generated by a fan and the heat conducted through the wall. An estimated value of the mol fraction of methane in transonic cryogenic testing is about 5 % at the highest. Note that this rarefactive action of the cryogenic tunnel is augmented as the jet temperature increases, because an extra amount of LN_2 is injected in the tunnel to remove the heat input of a jet gas.

Fig.3 represents the real-gas calculation of isentropic expansion pressure ratio, p/p_t, in the free stream for the case of P_t = 4bar and T_t = 150K. As shown, the saturation in the flow, shown by triangles, does not occur up to M = 1.9 and the deviation of p/p_t from the ideal diatomic value (reference) is very small throughout transonic Mach numbers. This is the case for the other isentropic flow parameters and normal shock parameters. The error of this magnitude can be considered negligible for the most wind-tunnel investigations.

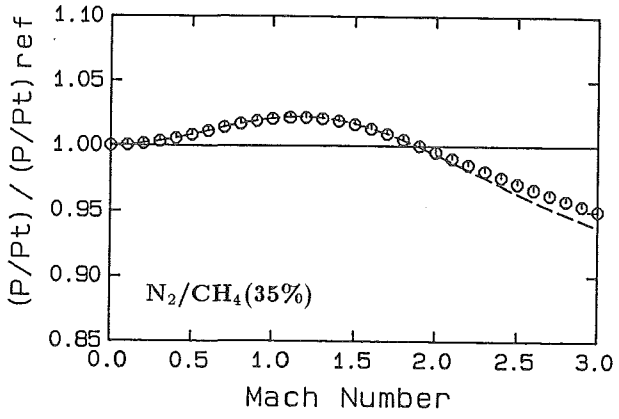

(a) p_{tj}=1600kPa, T_{tj}=500K (T_{tj}/T_{t0}=3.33)

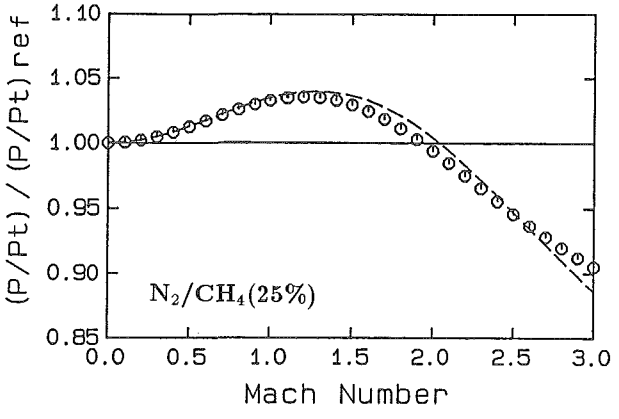

(b) p_{tj}=1600kPa, T_{tj}=750K (T_{tj}/T_{t0}=5.0)

Fig. 2 Isentropic expansion pressure ratio for N_2/CH_4

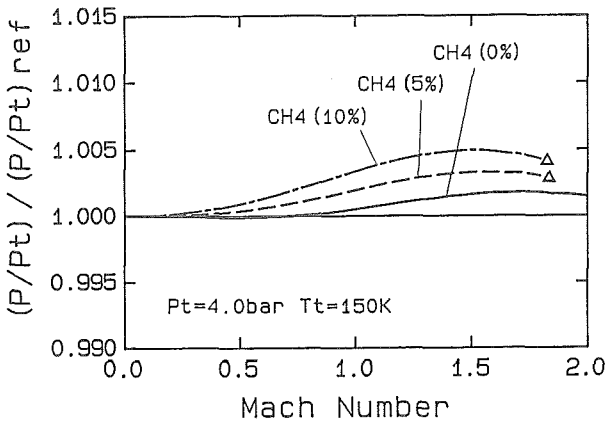

Fig. 3 Contamination effect of CH_4 on tunnel flow

3. Description of Experiments

3.1 Test Facility

The NAL 0.1m Transonic Cryogenic Wind Tunnel is a closed-circuit, fan-driven wind tunnel operated with nitrogen as the working gas. The tunnel is cooled by continuous LN_2 injection, and thermal insulation is attached to the tunnel external surface. At higher subsonic speeds, stagnation temperature can be varied from 90K to 150K with the maximum stagnation pressure up to 200 kPa. The test section is 0.1m squire and equiped with slotted top and bottom walls of 4% porosity and solid side walls. A detailed description of this wind tunnel and its operating performance is contained in Ref.8.

Injection of a jet gas has a great influence on the tunnel operation since its heat input is as much as 30% of the fan input power. Also, a helium jet causes an increase in sonic velocity and then affects free-stream Mach number. However, we have found that the automatic control system, based on a pair of personal computers, can regulate these disturbances caused by jet injection almost instantly. The tunnel pressure and temperature can be maintained within to 0.1 kPa and 0.1K of the set values, even when a jet gas is blowing. The indicated Mach number can be controlled within an accuracy of about 0.002.

3.2 Model

Fig. 4 shows a model installed in the test section of the 0.1 m TCWT. A cylindrical blunt-based nozzle afterbody model was used as a test article. This configuration was selected for the two reasons: (1) Only a small model of a simple configuration can be tested in the 0.1m test section. And, (2) a model of an identical afterbody configuration was previously tested by NACA with an ethylene/air combustor as a turbojet simulator (Ref.9).

The model is 150mm in length and 10mm in diameter. The forebody is a 18.9-degree cone-cylinder. The details of the nozzle and afterbody contour are shown in Fig.5. An exit diameter of the sonic nozzle is 3.5mm. The model was equiped with one pressure tap and one thermocouple in the base area. The base pressure was a primary measurement with which the effect of jet temperature was evaluated. This model is composed of thin SUS-304 pipes and assembled with silver brazing and soldering. A pitot tube and a thermocouple were provided inside the model to measure the stagnation condition of a jet gas. The model is strut-supported in the center of test section. The cross-section of the supporting strut is double-wedge having thickness ratio of 6.25%.

Two models of the same configuration were built and used in the tests. The first model (designated Model A) was dismissed after a number of hot-jet runs, because leakage of a jet gas occurred in the inner pipe. The second model of the same configuration (Model B) was built as a replacement for Model A. Small discrepancies in the measured base pressure data were found between the two models at near critical nozzle pressure ratios. Possibly, this is attributed to small geometrical differences in nozzle contour.

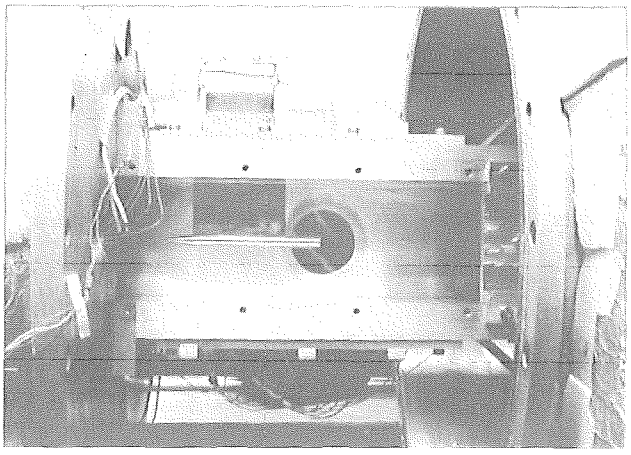

Fig. 4 Model installation in the NAL 0.1m TCWT

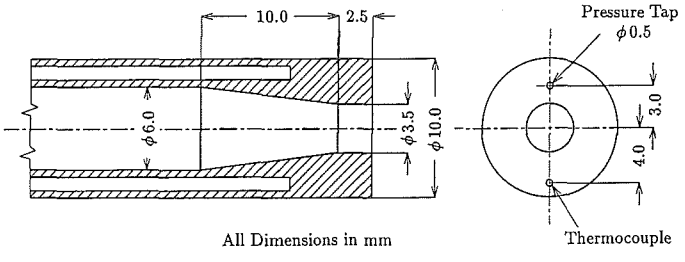

Fig. 5 Details of model afterbody configuration

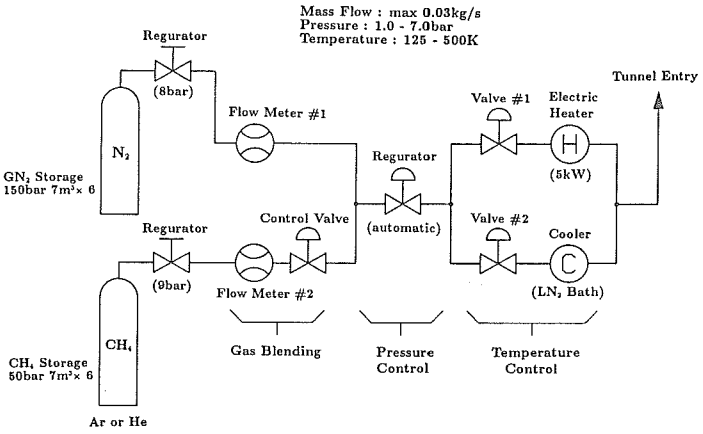

Fig. 6 Schematic diagram of jet gas supply system

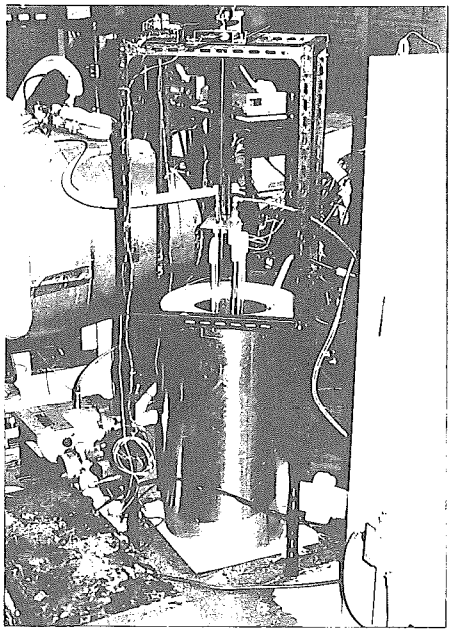

Fig. 7 Heat exchanger and LN_2 bath

3.3 Gas Supply System

In the present experiments, pure nitrogen and different mixtures of nitrogen and either of methane, argon, or helium were used as a test gas. Nominal purity of N_2, Ar, and He was 99.999% while that of CH_4 was 99.95%.

Fig.6 is a schematic diagram of a jet gas supply system. Gases stored in pressure cylinders are mol-controlled, pressure-regulated, temperature-conditioned, and supplied to the model. The gas blending system is based on a pair of mass-flow meters, both of which were calibrated by using a sonic venturi flow meter as a reference. The same gases as used in the wind tunnel tests were also used in the calibration test. The mol fraction of a component gas in the mixture can be varied from 0 to 90 percent by controlling a flow valve located in one of the two gas passages. An estimated accuracy in the measured mol fraction is better than 5%.

The temperature of a jet gas is controlled by an electric heater and a LN_2 bath (Fig.7). When the set point is higher than room temperature, jet temperature is controlled by changing the mixing ratio of a heated gas at 520 K through an electric heater and a gas bypassing the heater. When the set value is lower than ambient temperature, a gas was cooled by passing through a copper-tube manifold immersed in LN_2 bath. A fine control of the temperature is carried out by changing the depth of immersion. The minimum jet temperature (125K in our tests) was determined by the empirical formula of condensation onset for N_2. The control of pressure and temperature of a jet gas was made automatically and maintained within to 0.5kPa and 5K, respectively.

3.4 Test Conditions

Tests were primarily conducted at free-stream Mach number of 0.8, although some data were taken at Mach numbers of 0.6 and 0.9 too. The tunnel stagnation temperature ranged from 100 to 140 Kelvin, while the jet temperature was varied from 125K to nearly 400K, which provided the jet temperature ratio, T_{tj}/T_{t0}, up to 3.6 or higher.

The detailed test condition depends on the specific test objective:

CASE 1 : Confirmation of the Similarity Rule

Model ..... Model A
Mach number, M 0.8
Stagnation condition, (p_t, T_t) ..... (110kPa,100K), (144kPa,120K), and (181kPa,140K)
Reynolds number based on d_j ..... 7.0×10^5 (const.)
Jet gas ..... pure nitrogen
Nozzle pressure ratio, NPR ..... off to 6.0
Jet temperature ratio, TR ..... 1.25 and 3.0

CASE 2 : Effect of Jet Temperature Ratio

Model ..... Model B
Mach number, M ..... 0.6, 0.8 and 0.9
Stagnation pressure, p_t 110kPa
Stagnation temperature, T_t ..... 100K or 140K
Jet gas ..... pure nitrogen
Jet nozzle pressure ratio, NPR ..... off to 6.0
Jet temperature ratio, TR ..... 1.0 to 3.6 (or higher)

CASE 3 : Effect of Specific Heat Ratio

Model ..... Model B
Mach number, M ..... 0.6 and 0.8
Stagnation pressure, p_t 110kPa
Stagnation temperature, T_t 140K
Jet gas ..... mixtures of nitrogen and methane (or argon)
Mol fraction ..... 0 to 60% (50% in some cases)
Specific heat ratio, γ_j ..... 1.30 to 1.53
Jet nozzle pressure ratio, NPR ..... 2.0 to 6.0
Jet stagnation temperature, T_{tj} ..... 400K (TR=2.88)

CASE 4 : Effect of Gas Constant

Model ..... Model B
Mach number, M 0.8
Stagnation pressure, p_t 110kPa
Stagnation temperature, T_t 140K
Jet gas ..... mixtures of nitrogen and either of Ar or He
Mol fraction ..... 25% and 50%
Specific heat ratio ..... 1.44 and 1.50
Gas constant, R_j ..... 268 and 245J/kg-K for N_2/Ar
378 and 519J/kg-K for N_2/He
Jet nozzle pressure ratio, NPR ..... 2.0, 4.0, and 6.0
Jet stagnation temperature, T_{tj} ..... 200K, 300K, and 400K

3.5 Note on Data Reduction

It was found from real-gas calculations that, within the operational envelop of the NAL 0.1m TCWT, the free-stream properties such as Mach number and dynamic pressure could be calculated assuming a working gas was thermally perfect. Effects of mixing with a gas other than nitrogen was also accounted for in calculating the free-stream properties. The mol fraction of a foreign gas (CH_4, Ar, or He) in the free-stream was estimated from the mass flow measurements in the gas blending system and the LN_2 flow measurement by a turbine flow meter located in the LN_2 supply line.

4. Results and Discussions

4.1 Confirmation of the Similarity Rule

From a view point of the similarity rule, duplication of the absolute jet temperature is not essential, but duplication of the relative value of jet temperature to free-stream temperature, T_{tj}/T_{t0}, is important. Fig.8 (from Ref.6) represents the data obtained at three different temperature levels. The temperature of the free stream was varied from 100 to 140 Kelvin and the jet temperature was also varied in such a way that T_{tj}/T_{t0} was kept constant at 3.0. The Reynolds number was also kept constant in all cases by adjusting the pressure level. As shown, the base pressure data taken for three different temperature conditions are almost identical, as long as the value of T_{tj}/T_{t0} is maintained to a constant value. This observation confirms the basic similarity rule in hot-jet simulation.

4.2 Comparison with the Hot-Jet Data

In Ref.9, hot-jet results obtained by NACA for various afterbody configurations including one used for the present experiment are reported. The NACA tests were conducted in an atmospheric ambient-temperature tunnel using an ethylene/air combustor as a hot-jet simulator. Properties of the combustion products of ethylene and air are very similar to those of the actual turbojet exhaust gas since the H/C atom ratio of ethylene is the same as that for typical jet fuel. The base pressure data for jet temperatures of cold (about 298K), 700K and 922K are presented in this report. Over this range, the stagnation value of γ_j was varied from 1.4 to 1.33. Table 2 gives the properties of a test gas used in the cryogenic tests as compared with those for the NACA tests.

Figures 9(a) and 9(b) show a comparison of the base pressure data obtained from the cryogenic technique with that from the hot-jet technique. For the reason that will be explained later, the abscissa in this figure is the ratio of squire root of the product of gas constant, R_j, and jet temperature, T_{tj}, instead of the ratio of jet temperature to free-stream temperature. As is seen, a good qualitative agreement was found between the two data. Overall trends of C_{pb} variations with jet temperature are similar for both tests, although a significant difference in the pressure level is noted. This difference is believed to be attributed to the difference in model support system (strut-mounted versus wing-tip mounted).

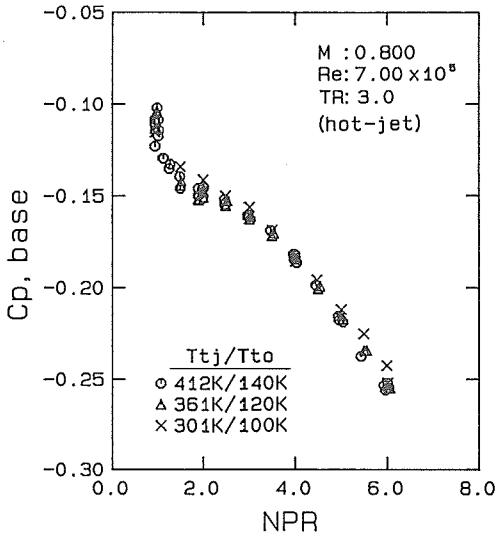

Fig. 8 Confirmation of similarity rule in hot-jet simulation

	M_0	T_{t0}	GAS	T_{tj} (TR)	γ_j
NACA	0.80	320K	air	298K (0.93)	1.40
	0.80	320K	C/P	700K (2.19)	1.36
	0.80	320K	C/P	922K (2.88)	1.33
PRESENT	0.80	140K	N_2	140K (1.00)	1.40
	0.80	140K	N_2/CH_4(40 %)	300K (2.14)	1.36
	0.80	140K	N_2/CH_4(40 %)	400K (2.86)	1.33

Table 2 Properties of a jet gas (present versus NACA)

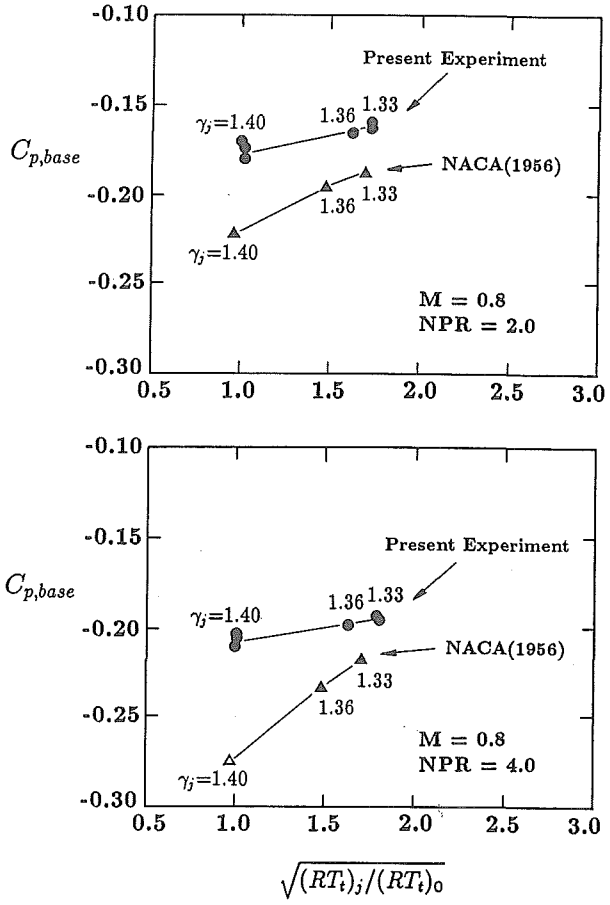

Fig. 9 Comparison of the cryogenic method with the hot-jet test

Figs.10(a) and 10(b) are examples of the Schlieren pictures taken in the present tests for both cold- and hot-jet conditions. For a hot jet, the mixing layer can be clearly observed as dark and bright zones, since the density gradient exists across the mixing layer. Because of limited quality of these pictures, the difference in jet plume shape between a N_2 jet and a N_2/CH_4 jet is not clear. A bright spot observed upstream of the model end is a gap in the model external junction caused by thermal expansion due to jet temperature. This gap appeared only in Model B and at high NPRs. Agreement of C_{pb} data at high NPRs between Model A and Model B shows that an influence of this gap on the overall phenomena can be negligible.

4.3 Effects of Jet Temperature Ratio

With the previous hot-jet simulation techniques using heated gases, it is difficult to determine the individual effect of jet temperature ratio since the value of γ varies simultaneously as gas temperature increases to 1000 Kelvin or higher. However, in a cryogenic wind tunnel, it is possible by using N_2 as a jet gas to isolate the effect of jet temperature ratio from that of specific heat ratio. Nitrogen is reported to behave like an ideal diatomic gas (γ=1.4) even at cryogenic temperatures (Ref.10).

Figures 11(a) to (c) show the effects of the jet temperature ratio on the base pressure at a constant nozzle pressure ratio for free-stream Mach numbers of 0.6, 0.8 and 0.9. The abscissa of this figure is again the ratio of the squire root of the product of R and T_t. This is actually equal to the ratio of the squire root of T_t, since both the tunnel and jet gases are pure nitrogen in this case (R_0=R_j).

As shown in Figs.11, the base pressure increases with increasing jet temperature. The variation in C_{pb} appears to be a linear function of the squire root of T_{tj}/T_{t0}. The slope is a weak function of nozzle pressure ratio. This trend is similar at all Mach numbers. The increase in C_pb with jet temperature ratio indicates that the jet entrainment reduces as jet temperature increases. This can be considered to be related to a decrease in density of a jet gas with increasing temperature.

4.4 Equivalence of R and T in Jet Entrainment Effect

It has been reported in Ref.11 that molecular weight (gas constant) of a jet gas has an significant effect on the after-

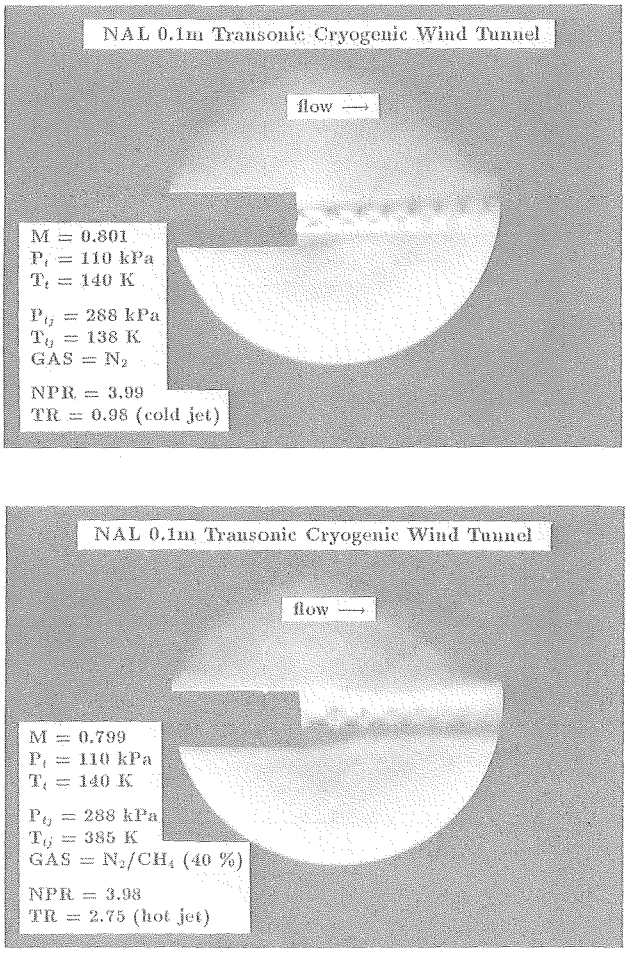

Fig. 10 Schlieren pictures for cold jet and hot jet

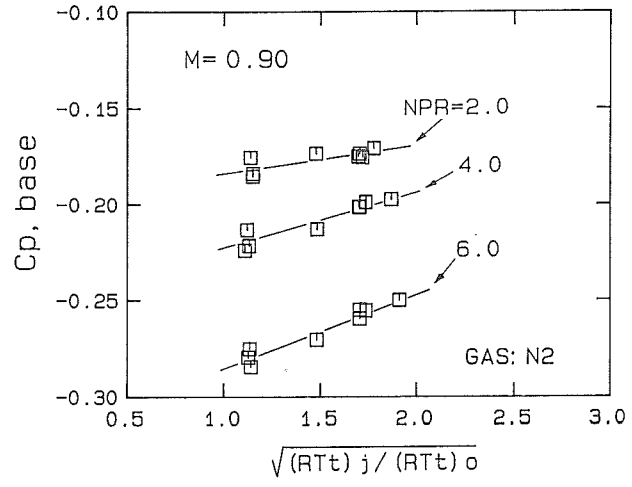

(a) M = 0.9

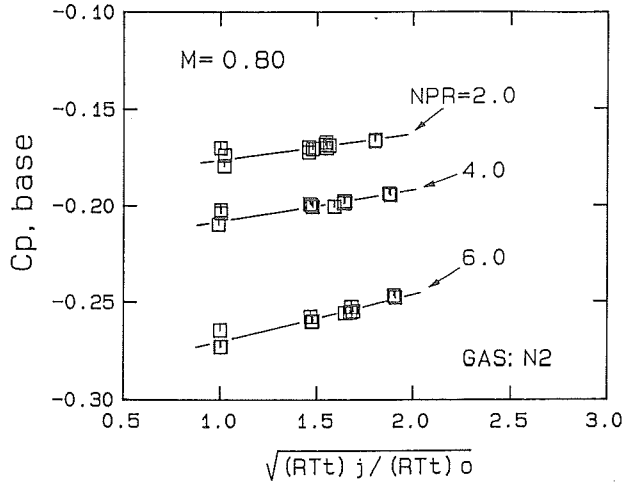

(b) M = 0.8

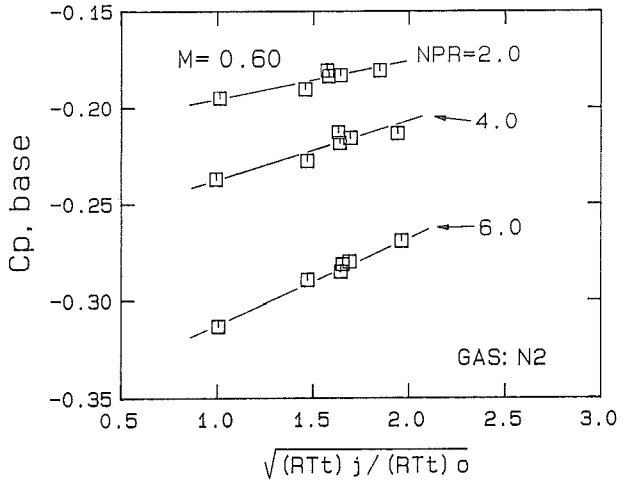

(c) M = 0.6

Fig. 11 Effect of jet temperature ratio on C_{pb}

body drag. By using differing mixtures by weight of N_2 and H_2 at ambient temperature as a test gas, they found that variation in gas constant has an effect similar to that caused by jet temperature variation. From these results, it has inferred in Ref.11 that the product of R_j T_{tj} relates drag effects produced by variations in either of these properties.

To the author's knowledge, this inference has not been verified to date, possibly due to difficulty in testing with heated gases. Through use of the cryogenic approach, however, it is very easy to verify this inference. We used differing mixtures of nitrogen and either of argon or helium as a jet gas for this purpose. Argon and helium have the same value of specific heat ratio (1.667) while the molecular weight of Ar (39.9) is larger by an order than that of He (4.0). Thus, use of argon or helium as a component of a jet gas allows a variation in gas constant (molecular weight) over the wide range.

Fig.12(a) indicates the results obtained using mixtures of nitrogen and either of argon (shown by circles) or helium (shown by triangles) having the mol fraction of 25%. This value of mol fraction corresponds to γ of 1.44. For these mixtures, gas temperature was also changed from 200K to 400K, which covered the jet temperature ratio from 1.43 to 2.88 (T_{t0}=140K). Similar results for the mol fraction of 50% (γ=1.50) are shown in Fig.12(b).

As is clearly seen in these figures, an identical change in C_{pb} occurred as a result of varying either of gas temperature or gas constant. This observation has verified that gas constant is equivalent to jet temperature in terms of its effect on the jet entrainment process. Note that C_{pb} for a constant NPR is directly proportional to the parameter, the ratio of the squire root of the product R T_t. This seems reasonable since either of both properties affects the mixing layer mass flux ratio. At a given specific heat ratio and a constant nozzle pressure ratio, the mass flux, ρV, is inversely proportional to the squire root of the R T_t product. The observation that C_{pb} increases with increasing the squire root of the product R T_t suggests that the jet entrainment reduces as the mass flux ratio decreases.

4.5 Separation of γ Effect and RT Effect

In addition to the effect of R and T_t on C_{pb}, that of the ratio of specific heats was also investigated. In this study, the value of γ_j was changed by mixing a nitrogen-based jet gas with either of methane (to reduce γ) or argon (to raise γ). Figures 13 and 14 show variations of the base pressure at a constant NPR with the mol fraction of an added gas, for CH_4 and Ar respectively. The jet temperature was kept constant at 400K while the free-stream temperature was 140K. As shown, increasing the mol fraction of CH_4 results in an increase in C_{pb}. The slope becomes smaller for higher NPRs. On the other hand, an increase in the mol fraction of Ar results in decreasing C_{pb} for NPRs of 2.0 and 4.0, while the trend is reversed at NPR of 6.0.

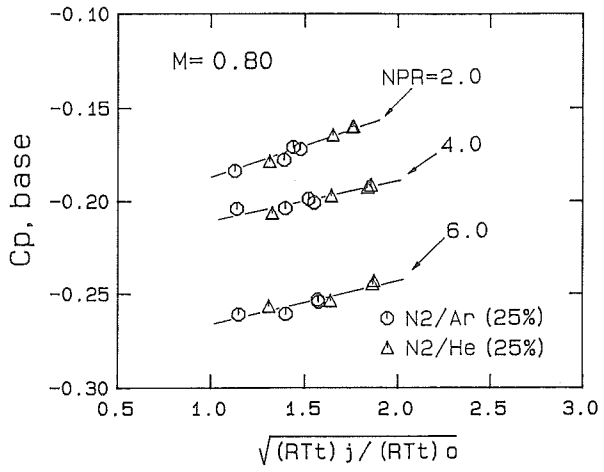

(a) mol fraction=25%, γ_j=1.44

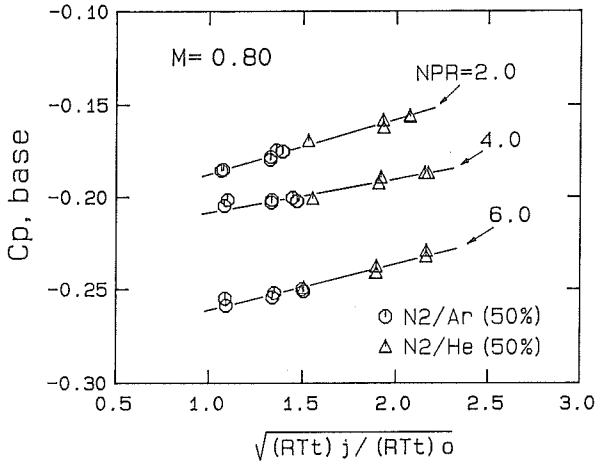

(b) mol fraction=50%, γ_j=1.50

Fig. 12 Equivalence of T_{tj} and R_j in the jet entrainment effect on C_{pb}

Fig.15 is the measured values of C_{pb} plotted as a function of γ of a jet gas. The value of γ ranges from approximately 1.30 to 1.53. However, it should be noted that this figure does not represent the independent effects of specific heat ratio on C_{pb}. Varying mol fraction is linked not only to γ but also to gas constant, since the molecular weight of CH_4 (16.0) and argon (39.9) is not the same as that of nitrogen (28.0). For example, a mixture of nitrogen and argon of 60% by mol has the value of gas constant smaller by 20% than that of pure nitrogen.

Consequently, the same data was plotted in Fig.16 as a function of the ratio of squire root of the RT_t product. In this figure, triangles, squires, and circles indicate data for N_2/CH_4, pure N_2, and N_2/Ar, respectively. The curves for a pure N_2 jet (appeared previously in Fig.10(b)) are also shown in this figure as solid lines. The value of γ is constant (1.40) and only the jet temperature varies along these solid lines. That is, these lines represent pure effects of the jet entrainment (RT_t effects). Therefore, any deviation in C_{pb} values from these solid lines shows the effect of γ isolated from that of gas constant.

As illustrated in Fig.16, the C_{pb} variations associated with changes in mol fraction of N_2/CH_4 or N_2/Ar mixtures are mostly resulting from a change in gas constant. This means that the jet entrainment effect is dominant in the jet interaction with the base flow. A variation in γ (from 1.30 to 1.53) results in only a residual effect on C_{pb}. Note here that this statement is valid only for the afterbody flow with large base areas and for relatively low NPRs. The situation may be reversed for smaller base areas or for higher NPRs, because the plume shape effects become significant for such cases.

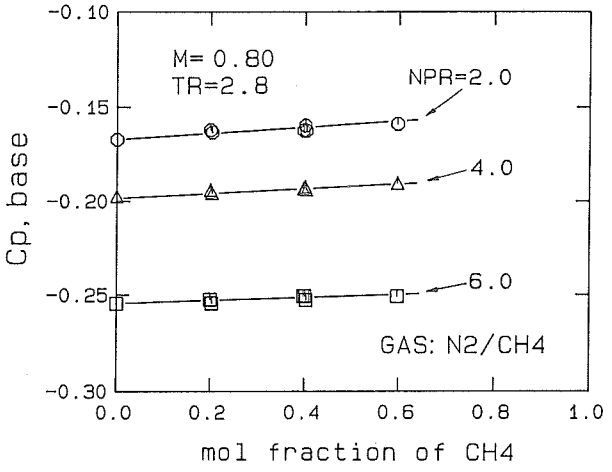

Fig. 13 Effects of mol fraction of CH_4 on C_{pb}

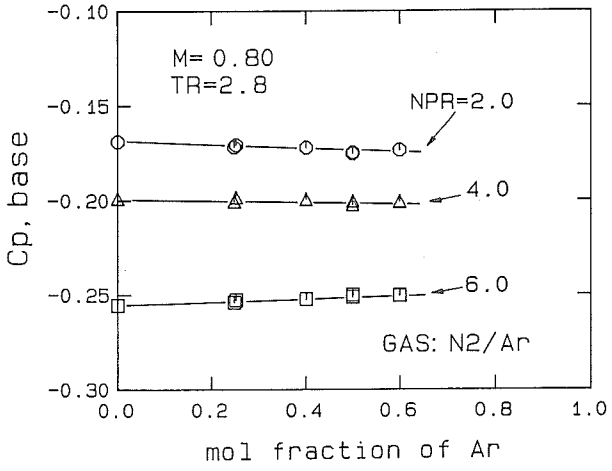

Fig. 14 Effects of mol fraction of Ar on C_{pb}

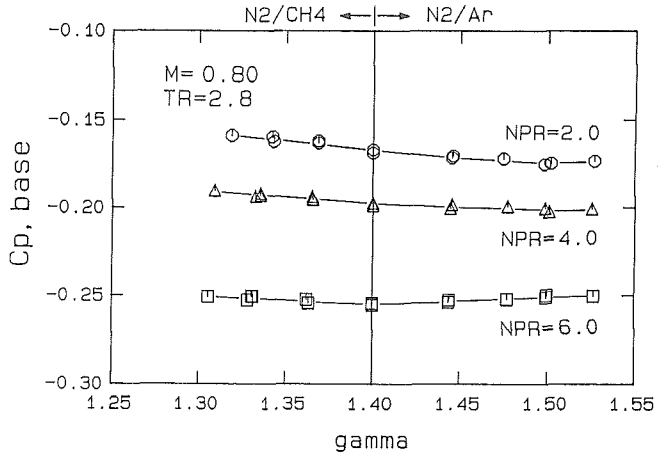

Fig. 15 Apparent variation in C_{pb} as a function of γ_j

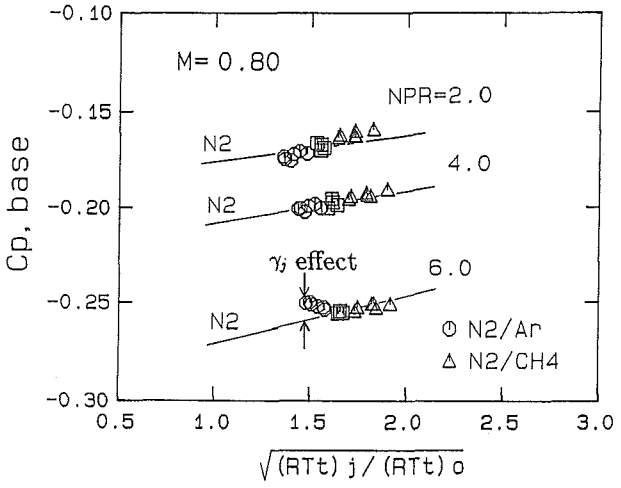

Fig. 16 Isolation of γ_j effects from RT effects

Note that the isolated effect of γ shown in Fig.16 varies depending on NPR. For NPR of 2.0, the base pressure decreases as the value of γ increases. On the other hand, at NPR=6.0, reducing γ increases the base pressure. At NPR of 4.0, there is no effect of γ. Usually, the effects of γ has been represented by the jet plume shape parameter like initial jet expansion angle or maximum plume diameter. The data shown in Fig.16 implies that variations solely in the jet plume shape parameter cannot give reasonable explanation to this observation. Further studies are needed for fully understanding the underlying physical phenomena.

5. Concluding Remarks

A novel hot-jet simulation technique, which utilizes the advantages of a cryogenic wind tunnel, has been presented. In order to validate this method, an experimental investigation was conducted in the NAL 0.1m Transonic Cryogenic Wind Tunnel. The data obtained by the cryogenic approach was compared with the previous hot-jet data. By varying the composition and the temperature of a jet gas, the independent determination of the effects of jet temperature ratio, specific heat ratio, and molecular weight (gas constant) on the base pressure was attempted. The obtained results can be summarized as follows:

(1) The base pressure data taken at three different tunnel temperatures, 100K, 120K, and 140K, are found to be practically identical as long as the ratio of jet temperature to free-stream temperature is maintained to a constant value. This observation has confirmed the basic similarity rule in hot-jet simulation.

(2) In a cryogenic wind tunnel, a real turbojet exhaust can be simulated with a mixture of nitrogen and methane at moderately elevated temperatures. Both the turbojet values of γ and T_{tj}/T_{t0} can be matched. The results obtained by the cryogenic method were found to be in good qualitative agreement with the previous hot-jet data obtained with an ethylene/air combustor.

(3) The base pressure decreases with increasing the jet temperature ratio. This indicates that the jet entrainment decreases as the jet temperature increases. This trend is similar for free-stream Mach numbers of 0.6, 0.8, and 0.9.

(4) By independent variations in either of gas constant and jet temperature, it has been verified that these two properties have an equivalent effect on the jet entrainment. The jet-entrainment effects on the base pressure are directly dependent on the squire root of the product of gas constant and jet temperature. This suggests that the mass flux ratio is a main parameter affecting the jet mixing process.

(5) For a blunt-based afterbody model used in this study, the jet entrainment accounts for the most of the observed jet temperature effects. Variations in γ have only a residual effect on the base pressure. The observed effect of γ cannot be explained reasonably by the jet plume shape parameter only. Further study on the underlying physical mechanism is necessary.

(6) As has been demonstrated in the present study, the cryogenic approach can provide an excellent tool for studying the jet-temperature-related effects at transonic Mach numbers. This technique is useful not only for the aircraft development tests but also for the fundamental research on the jet interaction.

Acknowledgements

The author would like to thank Dr. Hideo Sawada and Mr. Takeo Aoki of Aerodynamic Testing Techniques Lab. at NAL, for their continuing assistance in conducting experiments at the NAL 0.1m Transonic Cryogenic Wind Tunnel.

References

1. *Aerodynamics of Aircraft Afterbody* , AGARD AR-226, June 1986.

2. Compton, W. B., III, "Effects of Jet Exhaust Gas Properties on Exhaust Simulation and Afterbody Drag", NASA TR R-444, 1975.

3. Robinson, C. E., High, M. D., et al. "Exhaust Plume Temperature Effects on Nozzle Afterbody Performance over the Transonic Mach Number Range", AGARD CP-150, March 1975, pp.19-1 - 19.16.

4. Peters, W. L., " A Simulation Technique for Jet Temperature Effects on Nozzle -Afterbody Drag at Transonic Mach Numbers", AIAA-85-1463, July 1985.

5. Asai, K., "Hot-Jet Simulation in Cryogenic Wind Tunnels", NASA Reference Publication 1220, July 1989.

6. Asai, K. and Aoki, T., "Experiments to Evaluate Hot-Jet SImulation Capabilities in Cryogenic Wind-Tunnel Testing", AIAA-92-0567, Jan. 1992.

7. Asai, K., "Theoretical Evaluation of Test Gases for Use in Propulsion Simulation in Cryogenic Wind Tunnels", Proc. of The 23rd. Fluid Dynamics Conference in Japan, Nov. 1991.

8. Takashima K., Sawada H., et al., "Trial Manufacture of NAL 0.1m x 0.1m Transonic Cryogenic Wind Tunnel", NAL Technical Report 910, Aug. 1986 (in Japanese).

9. Henry, Jr. B. Z., et al., "Additional Results of an Investigation at Transonic Speeds to Determine the Effects of a Heated Propulsive Jet on the Drag Characteristics of a Series of Related Afterbodies", NACA RM L56G12, 1956.

10. Adcock, J. B., "Real-Gas Effects Associated with One-Dimensional Transonic Flow of Cryogenic Nitrogen", NASA TN D-8274, Dec. 1976.

11. Peters, W. L., " A Comparison of Jet Temperature Effects on Afterbody Drag with Those from Jet Molecular Weight and Nozzle Area Ratio Variations", AIAA-80-1161, June 1980.